Discontinuous Galerkin Methods for Non-Conservative Hyperbolic Partial Differential Equations

Jaap van der Vegt
Department of Applied Mathematics
Universiteit Twente

Enschede, The Netherlands

Joint work with Sander Rhebergen and Onno Bokhove

USTC Summer School, August 31 – September 4, 2020

Slurry and sediment transport in pipelines (LIC Engineering)

Mud flow on the slopes of Santiaguito volcano (US Geological Survey)

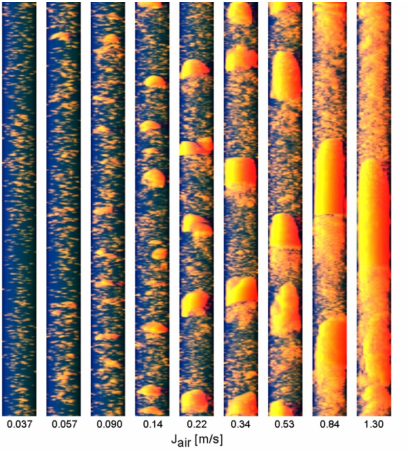

Various stages of bubbly flow, slug flow and churn-turbulent flow (Schleicher et al. Forschungszentrum Dresden-Rossendorf)

Motivation of Research

- Dispersed multiphase problems (e.g. mixtures of water and particles and/or bubbles) have too many relevant length scales, which can not all be captured in numerical simulations.
- The unresolved scales need to be modeled, which introduces a closure problem and requires insight in the relevant physical phenomena.

- An important effect of the modeling step can be that the mathematical structure of the problem changes.
- In particular, the conservation form of the equations may be lost.
- An interesting class of problems in dispersed multiphase and granular flows is for instance described by nonconservative hyperbolic partial differential equations.

Challenges

- The lack of the conservation property imposes several challenges:
  - In many of the dispersed flows (approximate) discontinuities can be develop (at least the level of the scales that can be represented in numerical simulations).

    This requires that we need an extension of the Rankine-Hugoniot jump relations to nonconservative hyperbolic pde's.
  - A similar problem with discontinuities occurs in discontinuous Galerkin finite element methods due to the element wise discontinuous approximation of the solution.

Objectives

- Our aim is to develop space-time discontinuous Galerkin discretizations that are suitable for both conservative and nonconservative partial differential equations

Overview of Presentation

- Overview of the main results of the theory of Dal Maso, LeFloch and Murat for nonconservative products
- Space-time DG discretization of nonconservative hyperbolic partial differential equations
- Numerical simulations of shallow two phase mixtures
- Conclusions

Non-Conservative Hyperbolic PDE's

- Nonconservative hyperbolic partial differential equations contain nonconservative products

$$\partial_t u + A(u)\partial_x u = 0$$

- The essential feature of nonconservative products is that $A \neq Df$, hence A is **not** the Jacobian matrix of a flux function f.

- This causes problems once the solution becomes discontinuous, because the weak solution in the classical sense of distributions then does not exist.

- This also complicates the derivation of discontinuous Galerkin discretizations since there is no direct link with the classical Riemann problem.

- **Alternative:** use the theory for nonconservative products developed by Dal Maso, LeFloch and Murat (DLM)

Non-Conservative Products

- Consider the function $u(x)$

$$u(x) = u_L + \mathcal{H}(x - x_d)(u_R - u_L), \quad x, x_d \in]a, b[,$$

with $\mathcal{H} : \mathbb{R} \to \mathbb{R}$ the Heaviside function.

- For any smooth function $g : \mathbb{R}^m \to \mathbb{R}^m$ the product $g(u)\partial_x u$ is not defined at $x = x_d$ since here $|\partial_x u| \to \infty$.

- Introduce a smooth regularization u^ε of u. If the total variation of u^ε, viz. $TV(u^\varepsilon) = \int_{(a,b)} |\frac{\partial u^\varepsilon}{\partial x}|$, remains uniformly bounded with respect to ε then Dal Maso, LeFloch and Murat (DLM) showed that

$$g(u)\frac{du}{dx} \equiv \lim_{\varepsilon\to 0} g\big(u^\varepsilon\big)\frac{du^\varepsilon}{dx}$$

  gives a sense to the nonconservative product as a bounded measure.

- The limit of the regularized nonconservative product depends in general on the path used in the regularization.

- Introduce a Lipschitz continuous path $\phi : [0,1] \to \mathbb{R}^m$, satisfying $\phi(0) = u_L$ and $\phi(1) = u_R$, connecting u_L and u_R in $\mathbb{R}^m$.

- The following regularization u^ε for u then emerges:

$$u^\varepsilon(x) = \begin{cases} u_L, & \text{if } x \in]a, x_d - \varepsilon[, \\ \phi(\frac{x - x_d + \varepsilon}{2\varepsilon}), & \text{if } x \in]x_d - \varepsilon, x_d + \varepsilon[, \\ u_R, & \text{if } x \in]x_d + \varepsilon, b[\end{cases} \qquad \varepsilon > 0.$$

- When ε tends to zero, then:

$$g(u^\varepsilon)\frac{du^\varepsilon}{dx} \rightharpoonup C\delta_{x_d}, \text{ with } C = \int_0^1 g(\phi(\tau))\frac{d\phi}{d\tau}(\tau)\,d\tau,$$

weakly in the sense of measures on $]a, b[$, where δ_{x_d} is the Dirac measure at x_d.

- The limit of $g(u^\varepsilon)\partial_x u^\varepsilon$ depends on the path ϕ.

- There is one exception, namely if an $q : \mathbb{R}^m \to \mathbb{R}$ exists with $g = \partial_u q$. In this case $C = q(u_R) - q(u_L)$.

DLM Theory

Dal Maso, LeFloch and Murat provided a general theory for nonconservative hyperbolic pde's.

- Introduce the Lipschitz continuous maps $\phi : [0,1] \times \mathbb{R}^m \times \mathbb{R}^m \to \mathbb{R}^m$ which satisfy the following properties:

(H1) $\phi(0; u_L, u_R) = u_L, \ \phi(1; u_L, u_R) = u_R,$

(H2) $\phi(\tau; u_L, u_L) = u_L,$

(H3) $\left|\frac{\partial \phi}{\partial \tau}(\tau; u_L, u_R)\right| \leq K|u_L - u_R|$, a.e. in $[0,1]$.

- **Theorem (DLM).** Let $u :]a, b[\to \mathbb{R}^m$ be a function of bounded variation and $g : \mathbb{R}^m \to \mathbb{R}^m$ a continuous function. Then, there exists a unique real-valued bounded Borel measure μ on $]a, b[$ with:

  1. If u is continuous on a Borel set $B \subset]a, b[$, then

  $$\mu(B) = \int_B g(u) \frac{du}{dx}$$

  2. If u is discontinuous at a point x_d of $]a, b[$, then

  $$\mu(\{x_d\}) = \int_0^1 g(\phi(\tau; u_L, u_R)) \frac{\partial \phi}{\partial \tau}(\tau; u_L, u_R)\, d\tau.$$

  By definition, this measure μ is the nonconservative product of $g(u)$ by $\partial_x u$ and denoted by $\mu = \left[g(u)\frac{du}{dx}\right]_\phi$.

Riemann Problem

- As essential element in the study of hyperbolic pde's is the Riemann problem

$$\frac{\partial u}{\partial t} + A(u)\frac{\partial u}{\partial x} = 0, \quad u(x,t) \in \mathbb{R}^p, x \in \mathbb{R}, t \geq 0$$

with initial solution

$$u(x,0) = \begin{cases} u_L, & \text{if } x < 0, \\ u_R, & \text{if } x > 0 \end{cases}$$

- **Theorem (DLM).** Assume that the solution u of the nonconservative hyperbolic pde is strictly hyperbolic with genuinely nonlinear or linearly degenerate fields.

  Let ϕ be a suitable Lipschitz continuous path which satisfies

$$\frac{\partial \phi}{\partial u_1}(1; u_0, u_0) - \frac{\partial \phi}{\partial u_1}(0; u_0, u_0) = Id, \quad \forall u_0 \in \mathbb{R}^p.$$

  Then, for $|u_L - u_R|$ small enough, the Riemann problem has a solution with bounded variation u which depends only on x/t and has the well known Lax structure.

  That is u consists of $p+1$ constant states separated by shock waves, rarefaction waves or contact discontinuities.

Rankine-Hugoniot Relations

- At the discontinuities the solution satisfied the generalized Rankine-Hugoniot relations which are equal to

$$-v(u^R - u^L) + \int_0^1 A(\phi_D(s, u^L, u^R))\partial_s \phi_D(s; u^L, u^R)ds = 0$$

  with ϕ_D a Lipschitz continuous path satisfying $\phi_D(0; u_L, u_R) = u_L$ and $\phi_D(1; u_L, u_R) = u_R$.

- For a conservative hyperbolic system of pde's, $\partial_t u + \partial_x f(u) = 0$ the Rankine-Hugoniot relations across a jump with u^L and u^R and velocity v reduce to

$$-v(u^R - u^L) + f(u^R) - f(u^L) = 0.$$

- The solution to the Riemann problem for a nonconservative hyperbolic system looks therefore like the well known solution to conservation laws.

- The only essential difference is the generalization of the Rankine-Hugoniot relations.

- Standard techniques to obtain (approximate) Riemann solvers for DG or finite volume methods can thus be applied as long as information about the path is known.

- In particular, the Rankine-Hugoniot relations are essential for the definition of the Non-Conservative Product (NCP) flux used in the DG discretization.

Path in Phase Space

- The solution to the Riemann problem, however, still depends on the path in phase space and is non-unique.

- The missing information should come from a parabolic regularization

$$\frac{\partial u}{\partial t} + A(u^{\epsilon})\frac{\partial u^{\epsilon}}{\partial x} = \epsilon \frac{\partial}{\partial x}\left(D(u^{\epsilon})\frac{\partial u^{\epsilon}}{\partial x}\right)$$

  where $D \geq 0$ is a smooth matrix-valued function.

- Consider the following traveling wave solutions to the Riemann problem

$$u^\epsilon = w^\epsilon(x - st) = w^\epsilon(y)$$

$$\lim_{y \to -\infty} w^\epsilon(y) = w_L, \quad \lim_{y \to -\infty} \frac{d}{dy} w^\epsilon(y) = 0$$
$$\lim_{y \to +\infty} w^\epsilon(y) = w_R, \quad \lim_{y \to +\infty} \frac{d}{dy} w^\epsilon(y) = 0$$

with s the wave speed.

- If we define $w : \mathbb{R}^p \to \mathbb{R}^p$ as

$$w(\frac{y}{\epsilon}) = w_\epsilon(y)$$

it satisfies the ordinary differential equation

$$(A(w) - s)w' = \big(D(w)w'\big)'$$

which does not depend on the parameter ϵ.

- We can now construct analogous to conservative hyperbolic pde's p half-curves ϕ_i, $1 \leq i \leq p$ connecting the different states in the Riemann problem which provides the paths in phase space.

- In practice, considering the complexity of the non-conservative hyperbolic pde's describing e.g. dispersed multiphase flows, this is a highly non-trivial task.

Space-Time Discontinuous Galerkin Method

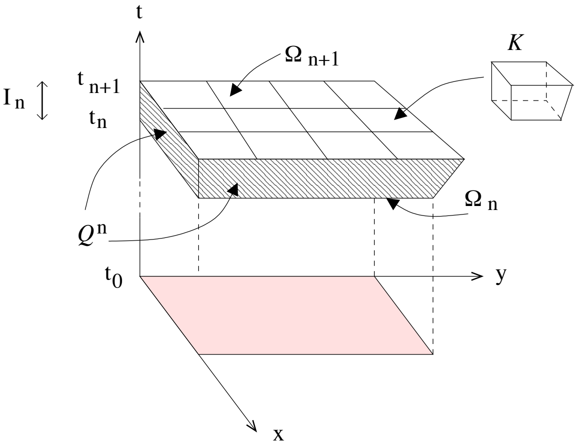

Sketch of a space-time mesh in a space-time domain.

Key Features of Space-Time DG Methods

- Simultaneous discretization in space and time: time is considered as a fourth dimension.

- Discontinuous basis functions, both in space and time, with only a weak coupling across element faces resulting in an extremely local, element based discretization.

- The space-time DG method is closely related to the Arbitrary Lagrangian Eulerian (ALE) method.

Benefits of Discontinuous Galerkin Methods

- Due to the extremely local discretization DG methods provide optimal flexibility for
  - achieving higher order accuracy on unstructured meshes
  - *hp*-mesh adaptation
  - unstructured meshes containing different types of elements, such as tetrahedra, hexahedra and prisms
  - parallel computing

Benefits of Space-Time Framework

- A conservative discretization is obtained on moving and deforming meshes.
- No data interpolation or extrapolation is necessary on dynamic meshes, at free boundaries and after mesh adaptation.

Disadvantages of Space-(Time) DG Methods

- Algorithms are generally rather complicated, in particular for elliptic and parabolic partial differential equations
- On structured meshes DG methods are computationally more expensive than finite difference and finite volume methods.
- The space-time DG method generally results in an implicit formulation which requires the solution of a large system of algebraic equations.

Space-Time Domain

- Consider an open domain: $\mathcal{E} \subset \mathbb{R}^d$.
- The flow domain $\Omega(t)$ at time t is defined as:

$$\Omega(t) := \{x \in \mathcal{E} \mid x_0 = t,\ t_0 < t < T\}$$

- The space-time domain boundary $\partial\mathcal{E}$ consists of the hypersurfaces:

$$\begin{aligned} \Omega(t_0) &:= \{x \in \partial\mathcal{E} \mid x_0 = t_0\}, \\ \Omega(T) &:= \{x \in \partial\mathcal{E} \mid x_0 = T\}, \\ \mathcal{Q} &:= \{x \in \partial\mathcal{E} \mid t_0 < x_0 < T\}. \end{aligned}$$

- The space-time domain is covered with a tessellation $\mathcal{T}_h$ consisting of space-time elements $\mathcal{K}$.

Discontinuous Finite Element Approximation

- The finite element space associated with the tessellation $\mathcal{T}_h$ is given by:

$$W_h := \left\{ W \in (L^2(\mathcal{E}_h))^m \;:\; W|_{\mathcal{K}} \circ G_{\mathcal{K}} \in (P^k(\hat{\mathcal{K}}))^m, \quad \forall \mathcal{K} \in \mathcal{T}_h \right\}$$

- The jump of f at an internal face $\mathcal{S} \in \mathcal{S}_I^n$ in the direction k of a Cartesian coordinate system is defined as:

$$[\![f]\!]_k = f^L \bar{n}_k^L + f^R \bar{n}_k^R,$$

with $\bar{n}_k^R = -\bar{n}_k^L$.

- The average of f at $\mathcal{S} \in \mathcal{S}_I^n$ is defined as:

$$\{\!\{f\}\!\} = \tfrac{1}{2}(f^L + f^R).$$

Space-Time DG Formulation of Nonconservative Hyperbolic PDE's

- Consider the nonlinear hyperbolic system of partial differential equations in nonconservative form in multi-dimensions:

$$\frac{\partial U_i}{\partial t} + \frac{\partial F_{ik}}{\partial x_k} + G_{ikr}\frac{\partial U_r}{\partial x_k} = 0, \quad \bar{x} \in \Omega \subset \mathbb{R}^q,\ t > 0,$$

  with $U \in \mathbb{R}^m$, $F \in \mathbb{R}^m \times \mathbb{R}^q$, $G \in \mathbb{R}^m \times \mathbb{R}^q \times \mathbb{R}^m$

- These equations model for instance bubbly flows, granular flows, shallow water equations and many other physical systems.

Weak Formulation

- Weak formulation for nonconservative hyperbolic system on space-time mesh

  Find a $U \in V_h$, such that for $V \in V_h$ the following relation is satisfied

$$
\begin{aligned}
&\sum_{\mathcal{K}\in\mathcal{T}_h} \int_{\mathcal{K}} V_i\big(U_{i,0} + F_{ik,k} + G_{ikr} U_{r,k}\big)\, d\mathcal{K} \\
&+ \sum_{\mathcal{K}\in\mathcal{T}_h} \left(\int_{K(t_{n+1}^-)} \widehat{V}_i (U_i^R - U_i^L)\, dK - \int_{K(t_n^+)} \widehat{V}_i (U_i^R - U_i^L)\, dK \right) \\
&+ \sum_{\mathcal{S}\in\mathcal{S}_I} \int_{\mathcal{S}} \widehat{V}_i \left(\int_0^1 G_{ikr}(\phi(\tau; U^L, U^R)) \frac{\partial \phi_r}{\partial \tau}(\tau; U^L, U^R)\, d\tau\, \bar{n}_k^L \right) d\mathcal{S} \\
&- \sum_{\mathcal{S}\in\mathcal{S}_I} \int_{\mathcal{S}} \widehat{V}_i [\![F_{ik} - v_k U_i]\!]_k\, d\mathcal{S} = 0
\end{aligned}
$$

Relation with STDG Formulation of Conservative Hyperbolic PDE's

- **Theorem 2.** If the numerical flux $\hat{V}$ for the test function V is defined as:

$$\widehat{V} = \begin{cases} \{\!\{V\}\!\} & \text{at } \mathcal{S} \in \mathcal{S}_I, \\ 0 & \text{at } K(t_n) \subset \Omega_h(t_n) \quad \forall n \geq 0, \end{cases}$$

then the DG formulation will reduce to the conservative space-time DG formulation when there exists a Q, such that $G_{ikr} = \partial Q_{ik}/\partial U_r$.

- After the introduction of the numerical flux $\hat{V}$ and integration by parts we obtain the weak formulation:

$$
\begin{aligned}
&\sum_{\mathcal{K}\in\mathcal{T}_h}\int_{\mathcal{K}}\left(-V_{i,0}U_i - V_{i,k}F_{ik} + V_i G_{ikr}U_{r,k}\right)d\mathcal{K}\\
&+\sum_{\mathcal{K}\in\mathcal{T}_h}\left(\int_{K(t_{n+1}^-)} V_i^L U_i^L\,dK - \int_{K(t_n^+)} V_i^L U_i^L\,dK\right)\\
&+\sum_{\mathcal{S}\in\mathcal{S}_I}\int_{\mathcal{S}}(V_i^L - V_i^R)\{\!\{F_{ik} - v_k U_i\}\!\}\bar{n}_k^L\,d\mathcal{S}\\
&+\sum_{\mathcal{S}\in\mathcal{S}_B}\int_{\mathcal{S}} V_i^L(F_{ik}^L - v_k U_i^L)\bar{n}_k^L\,d\mathcal{S}\\
&+\sum_{\mathcal{S}\in\mathcal{S}_I}\int_{\mathcal{S}}\{\!\{V_i\}\!\}\left(\int_0^1 G_{ikr}(\phi(\tau;U^L,U^R))\frac{\partial\phi_r}{\partial\tau}(\tau;U^L,U^R)\,d\tau\,\bar{n}_k^L\right)d\mathcal{S} = 0
\end{aligned}
$$

Numerical Fluxes

- The fluxes at the element faces do not contain any stabilizing terms yet, both for the conservative and nonconservative part

- At the time faces, the numerical flux is selected such that causality in time is ensured
$$\widehat{U} = \begin{cases} U^L & \text{at } K(t_{n+1}^-) \\ U^R & \text{at } K(t_n^+) \end{cases} .$$

- The space-time DG formulation is stabilized using the NCP (Non-Conservative Product) flux
$$\widehat{P}_i^{nc} = \left(\{\!\{F_{ik} - v_k U_i\}\!\} + P_{ik}\right)\bar{n}_k^L$$

Nonconservative Product Flux

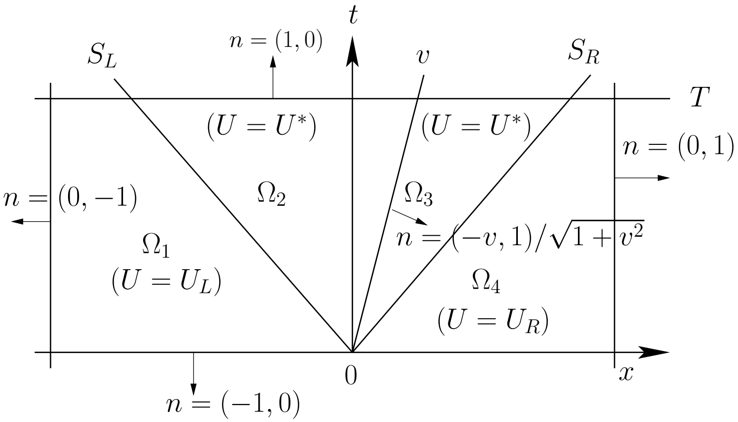

Wave pattern of the solution for the Riemann problem.

NCP Flux

Main steps in derivation of NCP flux:

- Consider the nonconservative hyperbolic system:

$$\partial_t U + \partial_x F(U) + G(U)\partial_x U = 0,$$

- Introduce the averaged **exact** solution $\bar{U}^*_{LR}(T)$ as:

$$\bar{U}^*_{LR}(T) = \frac{1}{T(S_R - S_L)} \int_{TS_L}^{TS_R} U(x, T)\, dx.$$

- Apply the Gauss theorem over each subdomain $\Omega_1, \cdots, \Omega_4$ and connect each subdomain using the generalized Rankine-Hugoniot relations.

- The NCP-flux is then given by:

$$\widehat{P}_i^{nc}(U_L, U_R, v, \bar{n}^L) = \begin{cases} F_{ik}^L \bar{n}_k^L - \frac{1}{2}\int_0^1 G_{ikr}(\bar{\phi}(\tau; U_L, U_R))\frac{\partial \bar{\phi}_r}{\partial \tau}(\tau; U_L, U_R)\, d\tau \bar{n}_k^L \\ \qquad \text{if } S_L > v, \\ \{\!\{F_{ik}\}\!\} \bar{n}_k^L + \frac{1}{2}((S_R - v)\bar{U}_i^* + (S_L - v)\bar{U}_i^* \\ -S_L U_i^L - S_R U_i^R) \\ \qquad \text{if } S_L < v < S_R, \\ F_{ik}^R \bar{n}_k^L + \frac{1}{2}\int_0^1 G_{ikr}(\bar{\phi}(\tau; U_L, U_R))\frac{\partial \bar{\phi}_r}{\partial \tau}(\tau; U_L, U_R)\, d\tau \bar{n}_k^L \\ \qquad \text{if } S_R < v, \end{cases}$$

- Note, if G is the Jacobian of some flux function Q, then $\widehat{P}^{nc}(U_L, U_R, v, \bar{n}^L)$ is exactly the HLL flux derived for moving grids in van der Vegt and van der Ven (2002).

Slope Limiters

- In case of discontinuities or large solution gradients two type of slope limiters have been tested:
  - For 1D test cases a minmod limiter is used
  - For 2D test cases a Hermite WENO limiter proposed by Luo et al. in combination with the Krivodonova discontinuity detector is used

Efficient Solution of Nonlinear Algebraic System

- The space-time DG discretization results in a large system of nonlinear algebraic equations:

$$\mathcal{L}(\hat{U}^n; \hat{U}^{n-1}) = 0$$

- This system is solved by marching to steady state using pseudo-time integration and multigrid techniques:

$$\frac{\partial \hat{U}}{\partial \tau} = -\frac{1}{\Delta t}\mathcal{L}(\hat{U}; \hat{U}^{n-1})$$

Numerical Simulations

Depth averaged two-fluid model

- The dimensionless depth-averaged two fluid model of Pitman and Le, ignoring source terms for simplicity, can be written as:

$$\partial_t U + \partial_x F + G\partial_x U = 0,$$

where:

$$U = \begin{bmatrix} h(1-\alpha) \\ h\alpha \\ h\alpha v \\ hu(1-\alpha) \\ b \end{bmatrix}, \quad F = \begin{bmatrix} h(1-\alpha)u \\ h\alpha v \\ h\alpha v^2 + \frac{1}{2}\varepsilon(1-\rho)\alpha_{xx} gh^2\alpha \\ hu^2 + \frac{1}{2}\varepsilon gh^2 \\ 0 \end{bmatrix}$$

$$G(U) = \begin{bmatrix} 0 & 0 & 0 & 0 & 0 \\ 0 & 0 & 0 & 0 & 0 \\ \varepsilon\rho\alpha gh & \varepsilon\rho\alpha gh & 0 & 0 & \varepsilon(1-\rho)\alpha_{xx} gh\alpha + \varepsilon\rho\alpha gh \\ \frac{2u^2\alpha}{1-\alpha} - \alpha u^2 - \varepsilon gh\alpha & -\varepsilon gh\alpha - \alpha u^2 & u(\alpha - 1) & u\alpha - \frac{2u\alpha}{1-\alpha} & (1-\alpha)\varepsilon gh \\ 0 & 0 & 0 & 0 & 0 \end{bmatrix}$$

- In the limit $\alpha \to 0$ the Pitmann and Le model reduces to the shallow water equations with ϵg akin to F^{-2}.

- In the limit $\alpha \to 1$ the Pitmann and Le model reduces to the Savage-Hutter model without source terms, which simulates avalanches of dry granular matter.

- **Note:** it can be proven that the space-time DG algorithm preserves the rest flow for the shallow water equations with a non-constant bottom topography when using linear basis functions and a linear path in phase space.

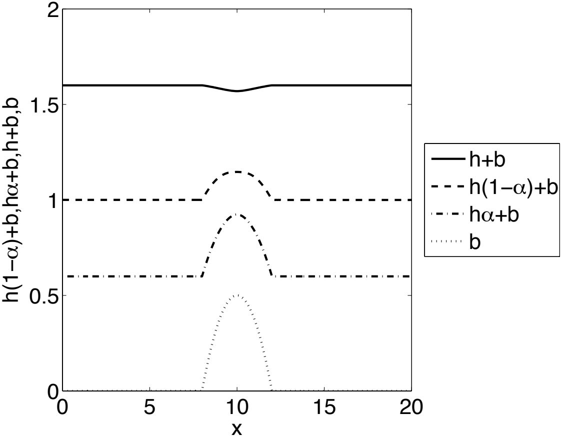

Steady-state solution for a subcritical two-phase flow (320 cells).

Total flow height $h+b$, flow height due to the fluid phase $h(1-\alpha)$, flow height due to solids phase $h\alpha$ and the topography b.

STDGFEM

N_{cells}	$h(1-\alpha)+b$ L^2 error	p	L^{max} error	p
40	$0.8171 \cdot 10^{-3}$	-	$0.2308 \cdot 10^{-2}$	-
80	$0.2025 \cdot 10^{-3}$	2.0	$0.5584 \cdot 10^{-3}$	2.0
160	$0.4871 \cdot 10^{-4}$	2.1	$0.1322 \cdot 10^{-3}$	2.1
320	$0.9789 \cdot 10^{-5}$	2.3	$0.2651 \cdot 10^{-4}$	2.3

N_{cells}	$hu(1-\alpha)$ L^2 error	p	L^{max} error	p
40	$0.3672 \cdot 10^{-4}$	-	$0.1442 \cdot 10^{-3}$	-
80	$0.5911 \cdot 10^{-5}$	2.6	$0.3448 \cdot 10^{-4}$	2.1
160	$0.1049 \cdot 10^{-5}$	2.5	$0.8471 \cdot 10^{-5}$	2.0
320	$0.1723 \cdot 10^{-6}$	2.6	$0.2078 \cdot 10^{-5}$	2.0

Error in $h(1-\alpha)+b$ for subcritical flow over a bump.

STDGFEM

	$h\alpha + b$			
N_{cells}	L^2 error	p	$L^{\max}$ error	p
40	$0.1404 \cdot 10^{-2}$	-	$0.4194 \cdot 10^{-2}$	-
80	$0.3537 \cdot 10^{-3}$	2.0	$0.9903 \cdot 10^{-3}$	2.1
160	$0.8511 \cdot 10^{-4}$	2.1	$0.2306 \cdot 10^{-3}$	2.1
320	$0.1712 \cdot 10^{-4}$	2.3	$0.4597 \cdot 10^{-4}$	2.3
	$hv(\alpha)$			
N_{cells}	L^2 error	p	$L^{\max}$ error	p
40	$0.1212 \cdot 10^{-4}$	-	$0.3409 \cdot 10^{-4}$	-
80	$0.1791 \cdot 10^{-5}$	2.8	$0.8054 \cdot 10^{-5}$	2.1
160	$0.3807 \cdot 10^{-6}$	2.2	$0.2048 \cdot 10^{-5}$	2.0
320	$0.5115 \cdot 10^{-7}$	2.9	$0.4861 \cdot 10^{-6}$	2.1

Error in $h\alpha + b$ and $hv\alpha$ for subcritical flow over a bump.

Two-phase dam break problem

The depth averaged model is used to compute a dam break problem with

$$U_L = \begin{bmatrix} 1.8 \\ 1.2 \\ 0 \\ 0 \end{bmatrix}, \quad U_R = \begin{bmatrix} 1.2 \\ 1.8 \\ 0 \\ 0 \end{bmatrix} \quad \text{where} \quad U = \begin{bmatrix} h(1-\alpha) \\ h\alpha \\ h\alpha v \\ hu(1-\alpha) \\ b \end{bmatrix}$$

where h is the flow depth, v the solid phase velocity, u fluid phase velocity, b bottom topography and α the volume fraction of the solid phase, with $\alpha_L = 0.4$ and $\alpha_R = 0.6$.

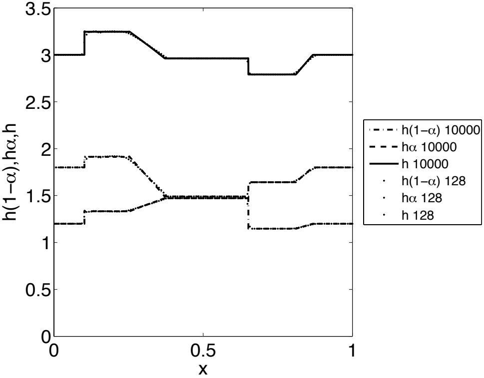

Two-phase dam break problem at time $t = 0.175$; mesh with 128 elements compared to mesh with 10000 elements. Solution of $h(1-\alpha)$, $h\alpha$ and h.

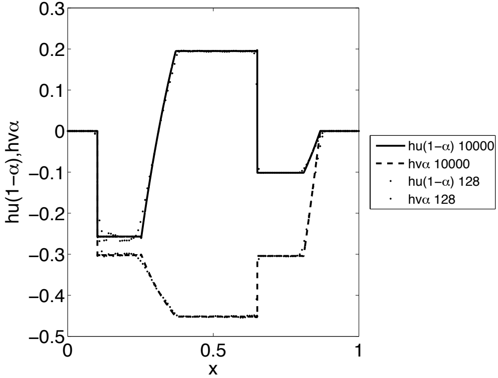

Two-phase dam break problem at time $t = 0.175$; mesh with 128 elements compared to mesh with 10000 elements. Solution of $hu(1-\alpha)$ and $hv\alpha$.

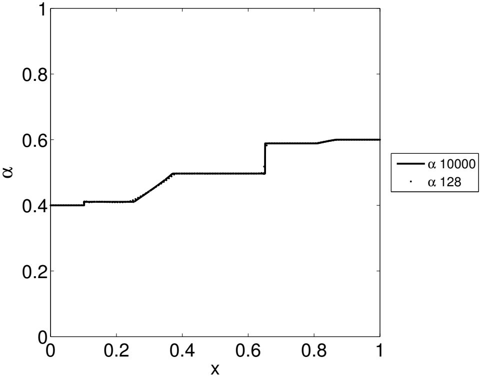

Two-phase dam break problem at time $t = 0.175$; mesh with 128 elements compared to mesh with 10000 elements. Solution of α.

Effect of Path in Phase Space

- Since it is generally very difficult to find analytic paths related to the parabolic regularized problem for realistic dispersed multiphase problems a large set of different paths was tested.

- For all shock cases tested the effect of the path is negligible, but one has to compute the path integrals accurately. Otherwise a significant path dependance is observed.

- For contact waves a path dependance is observed.

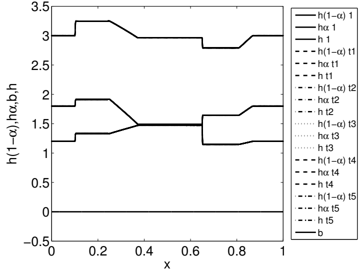

(a) The solution on whole domain.

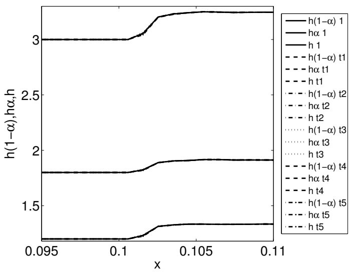

(b) The solution zoomed in on left shock wave.

Solution of $h(1-\alpha)$, $h\alpha$, b and h in two-phase dam break problem at time $t = 0.175$ calculated on a mesh with 1024 elements using Toumi paths.

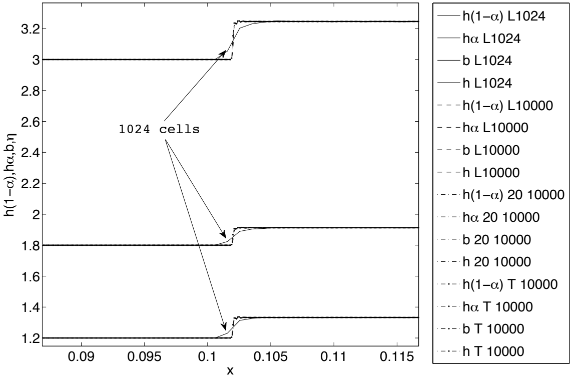

Zoom of $h(1-\alpha)$, $h\alpha$, b and h in left moving shock wave on a 10000 element mesh at $t = 0.175$ using the linear path, ϕ_{20v1} and the Toumi path ϕ_{T1}.

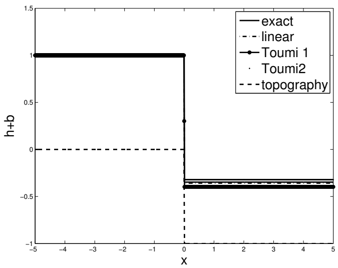

(c) Comparison of computed water level with exact solution

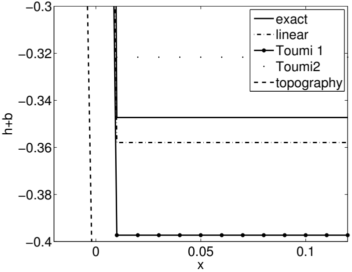

(d) Zoom of the water level right of the discontinuity in the topography.

Steady solution of contact discontinuity in shallow water equations related to the discontinuous topography on a mesh with 1000 elements (test case Parés and Castro).

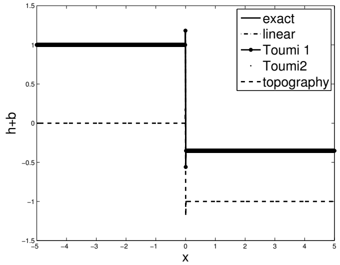

(e) Comparison of computed water level with exact solution

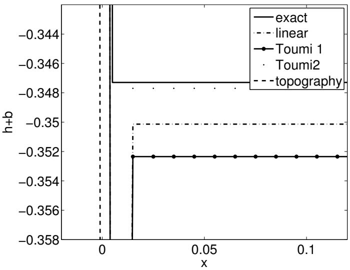

(f) Zoom of the water level right of the discontinuity in the topography.

Steady solution of contact discontinuity in shallow water equations related to the discontinuous topography on a mesh with 999 elements (test case Parés and Castro).

Flow through a Contraction

- Two-phase flow consisting of a mixture of solid particles in water. Experiments conducted by Bokhove and Akers.
- Flow features:
  - Solid particle density is slightly larger than that of water.
  - Initially the flow is started with a 5% particle volume fraction till steady state with oblique shocks is reached.
  - Next the flow is perturbed at the inlet by increasing the particle volume fraction to 30% for a brief period.
  - This changes the oblique shocks into an upstream moving shock and eventually a new steady state.
- The flow is simulated with a depth averaged model.

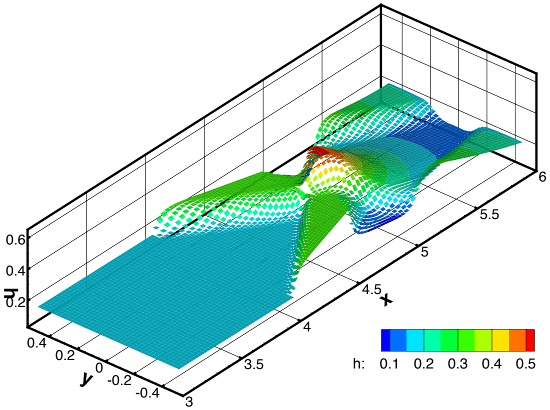

Oblique jump solution at $t = 22$.

Snapshot from the laboratory experiment at $t = 22$.

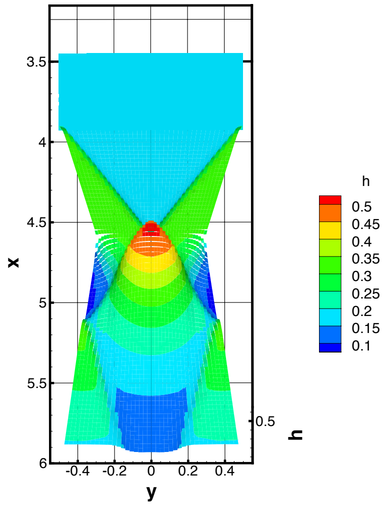

Top view of oblique jump solution at $t = 22$.

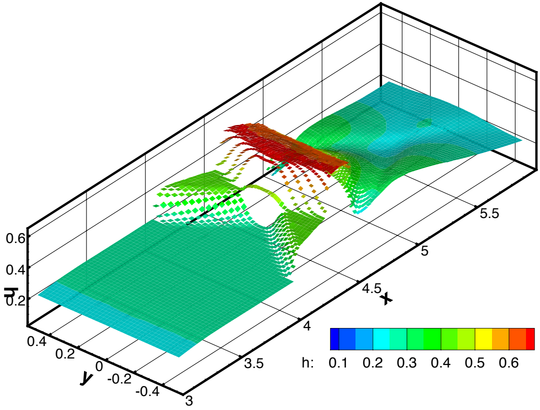

Transition phase at $t = 39$.

Snapshot from the laboratory experiment of the transition phase at $t = 39$.

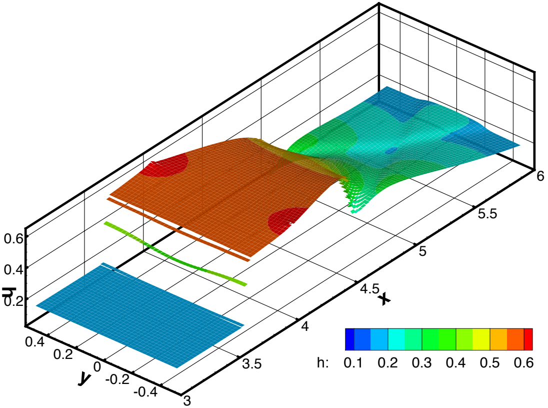

Upstream moving shock at $t = 100$.

Figure: *Upstream moving shock at* $t = 100$.

Conclusions

- A space-time DG discretization for nonconservative hyperbolic pde's using the DLM theory has been developed and tested.
- A new numerical flux for nonconservative hyperbolic pde's has been derived, which reduces to the HLLC flux for conservative pde's.
- The effect of the choice of the path in phase space is in practice for nearly all cases negligible except for steady contact discontinuities. It poses, however, interesting mathematical problems.
- The algorithm has been successfully tested on a depth averaged two-phase flow model and is applicable to a wide range of dispersed multiphase flow problems.

References

- S. Rhebergen, O. Bokhove and J.J.W. van der Vegt, Discontinuous finite element methods for hyperbolic nonconservative partial differential equations, JCP, Vol. 227, No. 3, pp. 1887-1922 (2008).

- S. Rhebergen, O. Bokhove and J.J.W. van der Vegt, Discontinuous finite element method for shallow two-phase flows, CMAME, Vol. 198, pp. 819-830 (2009).